33rd Annual International Conference of the IEEE EMBS
Boston, Massachusetts USA, August 30 - September 3, 2011

Wirelessly Powered Stimulator and Recorder for Neuronal Interfaces

Sudip Nag, *Student-Member, IEEE,* Dinesh Sharma, *Member, IEEE*
Electrical Engineering Department, Indian Institute of Technology Bombay, Mumbai, India
Email:sudip@ee.iitb.ac.in

Abstract— **Functional Electrical Stimulation (FES) is widely adopted in neuro-engineering to partially alleviate diseased functions in the brain, retina and cochlea. We present a 32-channel wirelessly powered constant current stimulator and low power recording amplifier for FES based applications. The biphasic stimulator utilizes innovative techniques for matched positive/ negative currents and thus improves charge balance. Electrode discharging scheme is added for stimulation artifact suppression. An improved low power amplifier is incorporated for evoked response measurements. Electrical performance is characterized using simulated electrode-electrolyte impedance. Closed-loop stimulation and recording experiments have been performed. Stimulation current magnitudes of 2µA-200µA and up to 400Hz rate have been realized. Theory and limitation of discharging scheme is explored while suppressing artifacts down to 3ms. Alternate anodic-first and cathodic-first stimulation pulses are adopted for enhanced charge balancing. The low power amplifier exhibits gain of 1200 and bandwidth 350Hz-1.02KHz. A multiplexer/ demultiplexer is used to share the front-end among 32 electrodes. The inductively coupled wireless energy harvester works at 125KHz-135KHz that can remotely deliver 1.4mW at 1cm distance to an equivalent of 10K load. The system can accommodate multielectrodes with impedance up to 100KΩ. The entire hybrid analog-digital system consumes 360µW quiescent power. Miniaturization makes it suitable for in-vivo applications.**

Keywords— *Neuro-stimulators, neuro-recorder, stimulation artifacts, charge balancing, wireless power.*

I. Introduction

Electrical charge injection for stimulation of neurons or cells is a well-known technique to evoke neuronal action potential (AP) spikes. Charge balanced biphasic current pulses are passed through the cell membranes that activate the ion channels and produce APs [1,2]. Functional Electrical Stimulation (FES) refers to the application of electrical stimulation to artificially restore limited functionality of neuronal systems, such as in diseased brain, retina or cochlea. Injecting threshold charges for stimulation is recommended for safe, long term and reliable operations in implantable neuro-prosthetic systems.

Recording of the neuronal responses [3] is essential to confirm the success of stimulations to evoke APs. Closed loop threshold calibration will help in optimal power utilization, prevent tissue heating and damages due to large electric fields. Successive stimulation and recording has a promising capability to calibrate the threshold stimulation charges. This threshold changes with impedance drifts in implantable multielectrodes [4] due to electrode degradation and scar tissue formation.

A closed loop system must be able to record evoked responses immediately after the termination of stimulation pulses. Residual voltages or stimulation artifacts are observed at the electrode terminals after the application of biphasic pulses [5,6]. Due to these, the high gain recording amplifiers saturate for several milli-seconds till the residual voltage is nearly nullified. Recording of short latency APs is thus hindered during the artifact periods. The stimulation artifacts must be suppressed within acceptable limits of 3 to 4ms [5] for a majority of applications. This enables advanced studies and applications in neuroscience.

Power delivery to the implantable system is a critical concern. Having a system with implantable batteries has the disadvantages of high cost, larger size and stringent safety requirements. Wireless powering by means of near-field inductive links has been shown to be advantageous [7,8]. An antenna in an in-vivo environment can harvest energy from another externally placed antenna. Therefore, it is preferable to use wirelessly powered implantable stimulators and recorders. Harvested power, range of operations and form factors may be optimized for specific neuronal applications and usage scenario.

We have demonstrated a low power neuro-stimulator and recorder architecture for charge balanced biphasic current injections and bandwidth limited amplification. A scheme of discharging the electrodes is employed to suppress stimulation artifact. Charge balancing is enhanced by alternate anodic-first or cathodic-first stimulation pulses. A low frequency near-field wireless power transfer scheme has been used. The same inductive coupler may also be used for bidirectional data transmission, instead of employing separate high frequency antennas, as in [9]. A low power microcontroller unit (MCU) based control logic has been incorporated for reconfigurable features and calibration. Simultaneous stimulation and recording experiments have been performed with equivalent electrode interface model. Miniaturization and power optimization in our system makes it suitable for long term in-vivo applications.

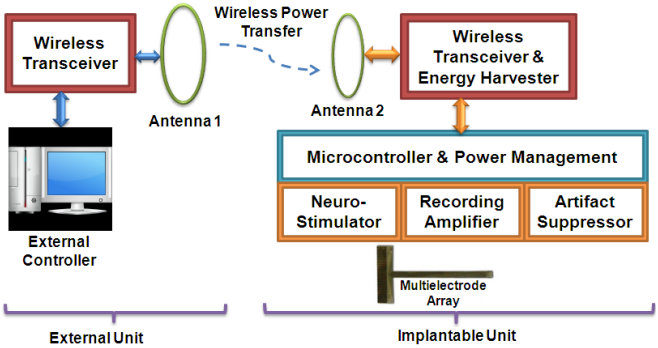

Figure 1: Block diagram of the energy harvested neuro-stimulator and recorder.

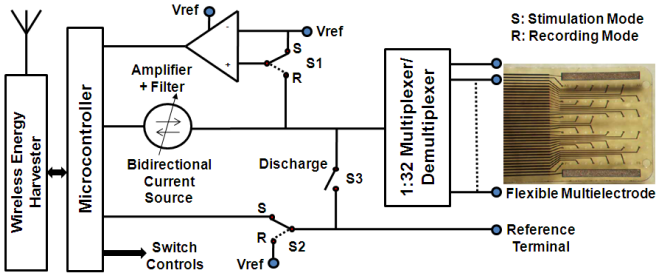

Figure 2: Functional block diagram of the system.

II. Neuronal Interface System

Figure 1 shows the system block diagram. An external controller or a personal computer (PC) is connected to the wireless transceiver and Antenna 1 to transfer power and data. The implantable unit consists of Antenna 2, transceiver, energy harvester, MCU, neuro-stimulator, recording amplifier and the artifact suppressor circuitry. Inductive coupling between Antenna 1 and 2 is possible while they are aligned correctly within few centimeters.

Figure 2 represents the functional architecture of the system. The switches S1 and S2 are kept in *S* positions during stimulation. The current source forces biphasic currents through the multielectrode channel selected by the multiplexer/ demultiplexer. The amplifier inputs are shorted and the switch S3 is open in *S* mode of operation. S3 is closed for up to few milliseconds after the stimulation current is forced to zero. This action will discharge any residual voltage across the stimulated electrode-electrolyte junction, which would otherwise generate a long artifact after high gain amplification. The recording mode is enabled by keeping S1 and S2 is *R* positions. The evoked responses from the neurons may be registered in this mode. The microcontroller governs the sequence and timing. The wireless energy harvester recovers inductively coupled power for battery-free and low-maintenance operation.

Figure 3 shows the schematic of the stimulator and the amplifier. The sub-sections are described below:

A. Neuro-stimulator

A bidirectional constant current source based stimulator circuit is realized using a single supply and digital controls. *Figure 3.a* shows the schematic of stimulator using a floating current source and conveyor switches. Current directions are controlled by means of analog switch positions. For positive load currents, switches S4 and S5 are connected to *+I* positions. Logic '*1*' on terminal *T1* and logic '*0*' on terminal *T2* activates positive load current. S4 and S5 are configured in *-I* positions for negative load current, while logic '*0*' in terminal *T1* and logic '*1*' on terminal *T2* are applied. Current magnitude is adjustable through a programmable resistor. Appropriate logic timing determines injected charges and balancing. This architecture helps in achieving better charge balance, since a single current source is used for positive and negative load currents. This avoids mismatch in current magnitudes and output impedance. The charge injection in each half phase is governed by the equation

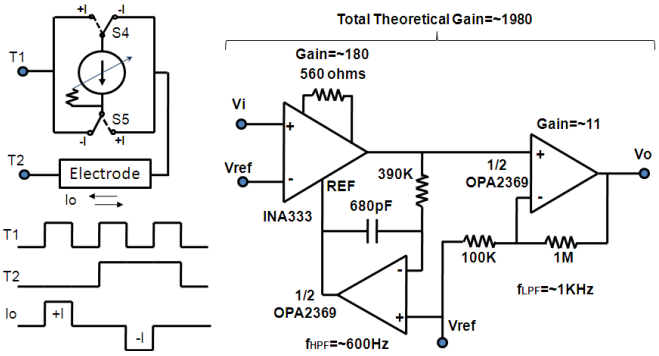

Figure 3 (a): Neuro-stimulator and (b) Amplifier.

$$Q = \frac{1}{2}\int_{t1}^{t2} I(t)\,dt = \frac{1}{2} I.(t2 - t1) \qquad (1)$$

Where Q is the injected charge, I is the stimulation current, *t1* and *t2* are starting and ending time of the half phase stimulation pulse.

LM334 chip is used as an adjustable constant current source. The chip works in source/sink mode without separate power supply terminals. TS3A24159 analog switches are used as current conveyors with low r_{ON} of 0.3Ω, for minimum *on-state* voltage drop and low charge injection of 9pC for suppressed feed-through.

The voltage compliance of the constant current sources is a limiting factor while operating at lower voltages and *VDD/2* as reference. During stimulation phases, the current conveyor switches and the digital control isolate the load from the *Vref* and thus increase the voltage compliance. Terminals *T1* and *T2* are tri-stated in recording mode.

B. Neuro-recorder

The recorder is essentially an amplifier with bandpass characteristics. *Figure 3 (b)* shows the simplified amplifier circuit. To reduce power consumption we have used low gain-bandwidth product amplifiers. By choosing the gain appropriately, we can use this stage as a low pass filter without an extra stage. AC coupled instrumentation amplifier (inamp) is used as a first order bandpass filter with gain. The low pass bandwidth of the inamp reduces to 1KHz at a gain of 180. The second gain stage is realized by the operational amplifier (opamp) based non-inverting amplifier. The non-inverting amplifier exhibits a low pass bandwidth of nearly 1.1KHz at a gain of 11. Total theoretical gain is thus 1980. An amplifier with first order high pass and second order low pass response is thus implemented. A reference voltage of 1.2V is used as *Vref*. During stimulation mode of operation, inputs of the inamp may be isolated from the load and shorted to *Vref* in order to reduce high gain output recovery time. INA333 inamp, OPA2369 opamps and TS5A2053 analog switches are used in this section.

C. Stimulation Artifact Suppressor

Stimulation artifact is defined as the time required by the recording amplifier's output to recover from saturation to baseline potential, without further saturation, after the last edge of stimulation pulse. Artifact suppression is realized by means of discharging the residual voltage at the electrode-

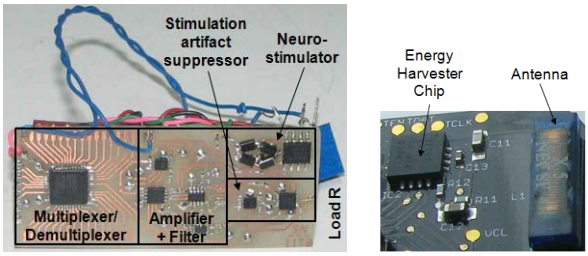

(a) (b)

Figure 4: (a) Analog front-end;
(b) Wireless power receiver circuit.

electrolyte interface. The electrode terminals are shorted for a brief period through an analog switch S3 (*figure 3*) after the application of stimulation pulses. The short is removed before the recording begins. First-order equivalent circuit (Randell's cell) during discharging is shown in *Figure 7* (inset). Discharge time constant is given by:

$$\tau_{Discharge} = \frac{\left(R_{sol}+R_{ON_{SW}}\right).R_t.C_{dl}}{R_{sol}+R_{ON_{SW}}+R_t} \quad (2)$$

Where, $\tau_{Discharge}$ is discharging time constant, R_{sol} is solution resistance, R_t is charge transfer resistance, C_{dl} is double layer capacitance, and $R_{ON_{SW}}$ is on-state resistance of the discharging switch. We may assume that after $5 \times \tau Discharge$ the baseline has settled to zero. A lower $\tau_{Discharge}$ is desirable for faster recovery. However, it is limited by the extracellular solution resistance R_{sol}.

Discharging causes additional current through the load that in turn disturbs charge balancing. Alternate anodic-first and cathodic-first stimulation pulses help in maintaining better charge balance while reducing artifacts. TS5A2066 analog switch is utilized in this section.

D. 32-Channel Multiplexer/Demultiplexer

A 1:32 multiplexer/demultiplexer has been used to share the stimulator and the recording circuits among thirty-two electrode channels. ADG732 chip is applied for matching channel to channel R_{ON} and low charge injection. A flex-connector is provided in this section for direct interface to flexible multielectrode, such as the FlexMEA36 (Multichannel Systems, Germany).

E. Wireless Energy Transfer

Inductive energy harvesting scheme is adopted to transfer power to the secondary side neuro-stimulator and the recorder circuits. A low frequency carrier in the range of 125 KHz to 135 KHz has been used in the present design. Low frequency circuit helps in increasing range and reducing dynamic power significantly. Longer range of operation is achievable due to larger depth of penetration at lower frequencies [10]. TMS3705 reader chip drives the primary coil and transmits power. Power is recovered through a secondary coil and TMS37157 transponder chip. The transponder is connected to the stimulator and the recorder circuits. The 2.66mH coils act as antennas. The reader side coil is usually bigger than the transponder coil for providing wider radiation field. The reader is powered from the USB

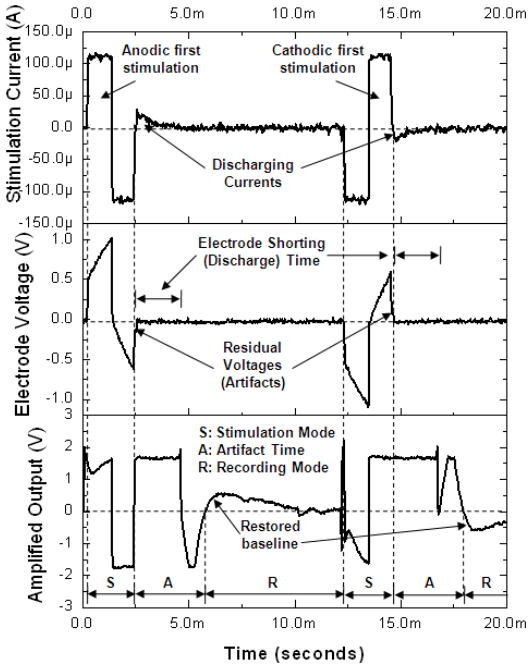

Figure 5: Stimulation and recording waveforms using simulated electrode-electrolyte interface.

port. The control commands are issued by a PC based user interface software.

F. Control Logic

Low power and very low frequency (12KHz) operated MCU is used to manage the timing and sequencing. The MCU selects the electrode of interest, controls stimulation current magnitudes, current directions, pulse durations, and switch operations. Power management is also governed by the same MCU.

Figure 4 (a) shows the printed circuit board (PCB) of the prototype of wirelessly powered neuro-stimulator and recorder unit. *Figure 4 (b)* shows the energy harvester section. Discrete surface mount components are used for this space constrained design. Commercially available components are chosen for rapid prototyping and lower cost.

III. Results & Discussions

We present the characterization results of the sub-sections and measurement results with simultaneous stimulation and recording. A first-order quasi-static load using resistor-capacitor (R-C) is used as a simulated or equivalent electrode-electrolyte interface.

Figure 5 shows stimulated constant currents, electrode voltages and amplifier output waveforms. During first phase of all constant current stimulation, corresponding voltage trace shows initial rise due to drop across R_{sol}, followed by a capacitive charging (C_{dl}). The second phase charges the electrode in opposite direction as current is reversed. Discharging currents are evident due to electrode shorting action for artifact suppression (*figure 5*, uppermost trace). Such extra load currents tend to disturb the charge balance at the load, even if the stimulator signals are ideal. Alternate

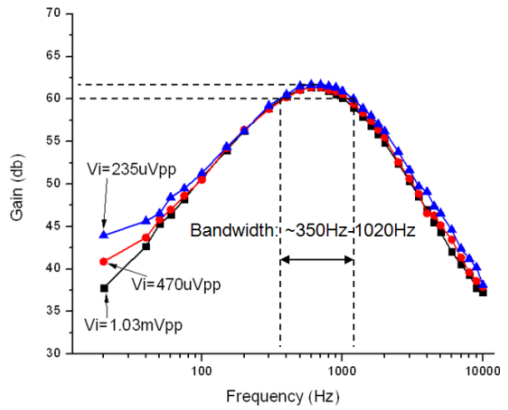

Figure 6: Frequency response of the amplifier.

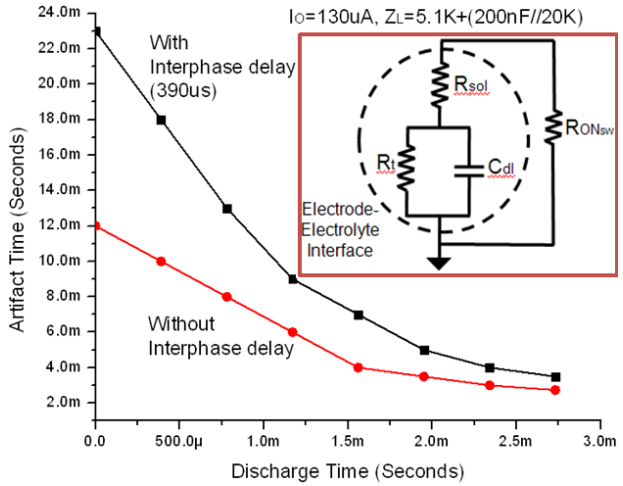

Figure 7: Stimulation artifact time as function of electrode discharge time and inter-phase delay. (Inset showing the equivalent circuit during electrode discharging)

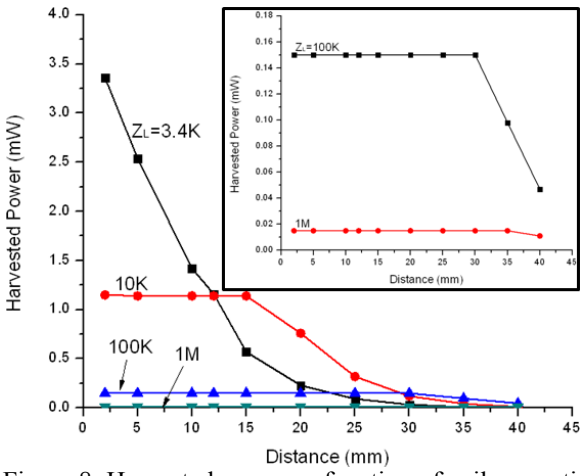

Figure 8: Harvested power as function of coil separation distance and load impedance.

anodic-first and cathodic-first stimulation pulses effectively solve this problem due to alternate discharging current polarities. However, alternate stimulation is not applicable in all cases, as the inverting pulse may trigger a different neural structure. The recording amplifier output resumes close to base line potential in less than 3ms for 2ms electrode shorting.

TABLE I
ELECTRICAL SPECIFICATIONS

SECTIONS	PARAMETERS	VALUES
Neuro-stimulator	Magnitude	2µA-200µA (16 steps)
	Rate	Up to 400Hz
	V-compliance	±2V (at load) for 3.4V supply
	Charge balancing (pulse-to-pulse matching)	~0.01% (Biphasic constant currents and alternate anodic/ cathodic first pulses)
Amplifier	Gain	~1200
	Bandwidth	350Hz-1.02KHz
Artifact Suppressor	Method	Electrode discharging
	Artifact Duration	Down to 2.8ms
Wireless Energy Harvester	Principle	Inductive (near-field)
	Carriers	125KHz and 134.2KHz
	Harvested Power	~1.4mW at 1cm separation (Z_L=10K)
	Data rate	8kbps (designed)
	Regulated supply	3.4V DC
System Power	Quiescent power	~360µW
	Overhead power	~90µW (stimulation at 100Hz)

Figure 6 shows the measured frequency response of the recording amplifier. The maximum measured gain is 61.6db as against of theoretical 65.93db. Similarly, the practical high pass cut-off is 350Hz, as opposed to 600Hz. Due to the overlap of high pass and low pass frequency responses the maximum gain reduces and the bandwidth is modified from the calculated values. The measured maximum gain is nearly 1200 and the bandwidth ranges between 350Hz and 1020Hz. AP's spectral distribution lies between 400Hz and 2KHz [11]. A partial sacrifice in bandwidth is justifiable as the temporal location of AP spikes are important than the actual shape. Smaller bandwidth for acquisition is helpful to reduce power, enables use of slower analog-digital converters (ADCs) and thus shortens memory buffers. The gain of 1200 is suitable to register few hundreds of micro-volts using an extra-cellular electrode and internal ADC inside MCUs. Input referred baseline noise of the amplifier system is between 2µV to 4µV.

Figure 7 shows the temporal characteristics of the discharging based stimulation artifact suppression with and without inter-phase delays in the stimulation pulses. Longer discharging time reduces artifact duration and vice-versa. Interphase delays facilitate self discharging of capacitor C_{dl}, through R_t. This results in larger residual voltages at the end of the stimulation pulses, causing longer artifacts. The inset shows the equivalent circuit during discharging. The low switch resistance $R_{ON_{SW}}$ shorts the electrode to the reference potential and discharges the interfacial capacitance C_{dl}. This helps in faster restoration of amplified baseline. Efficacy of the discharging scheme also depends on the rate of stimulation, especially at high frequencies. The present system is tested up to 100Hz stimulation rates.

Figure 8 shows harvested power with the low frequency wireless powering scheme. The reader and the transponder coils were aligned in air without absorbing bio-samples. The resistor loads were connected at the output of regulated DC voltage of 3.4V in the transponder side. Regulation is

maintained over longer range for larger resistive loads and vice-versa. Smaller resistance can accept more power at short distance. However, the accepted power drops sharply with distance. The harvested power is proportional to the transmitted power and the coupling parameters. Testing of the inductive coupling has also been done by placing human fingers between the coils separated by 15mm.

The electrical specifications are mentioned in the Table I. A 10KΩ load can draw nearly 1.4mW power at 1cm distance. The quiescent power drawn from the energy harvester unit is 360µW, while the transponder, MCU and the recording circuits are active. An additional 90µW (average) is consumed as overhead power while delivering approximately 251µW to load impedance at 100Hz stimulation rate (100µA for 2.45ms, to a 25.1K load). This can easily be provided by the wireless coupling with good regulation, as evident from *figure 8*. Measures are adopted to reduce circuit size, power and complexity without sacrificing precision performance and reliability. The PCB size is 36mm×16mm×2.2mm.

The calibration of stimulation threshold may be incorporated by means of repeated stimulation and measuring evoked responses with biological tissues. An increasing magnitude of currents may be applied with fixed pulse width and the neuronal responses can be noted. The minimum current value that evokes repeatable AP spikes may be noted on a software table. Such calibration procedure must be repeated for all electrode channels. Periodic recalibration is suggested to readjust the optimal stimulation parameters. Such close loop system is highly effective to utilize power efficiently. It also enhances safety and reliability in long term neuronal implants.

The reported system can be used with Asynchronous Interleaved Sampling (AIS) algorithm [12] to select the stimulation channels in real time. Such Bio-inspired algorithm will be highly effective to reduce inter-electrode cross-talks and power losses.

Miniaturization and biocompatibility are extremely important factors for implantable systems. Single chip integration is possible for size reduction. Flexible PCBs will also help to reduce volume of the system. Biocompatibility may be obtained by coating the circuit board with polydimethylsiloxane (PDMS) polymer.

IV. Conclusions

An innovative architecture for wirelessly powered 32-channel neuronal interface is demonstrated. The system uses commercially available miniature components for lower cost (<$100), fast prototyping and easy replication. A new architecture of the programmable biphasic constant current stimulator is presented using a floating current source and conveyor switches. This reduces overhead power and achieves better charge balancing as compared to conventional voltage-to-current converter based stimulators. The time constant has been modeled for electrode discharge based stimulation artifact suppression. Discharging, which causes charge unbalancing at the load, is further compensated by optional alternate anodic-first and cathodic-first stimulation pulses. Temporal performance characteristic of the discharging scheme is shown with simulated electrode-electrolyte interface. An efficient gain-determined band-limited amplification scheme is adopted for very low power neuronal signal pick-up. Performance of the inductively coupled wireless energy harvester is characterized for varied load impedance and distance between coils. Stimulation and recording experiments with electrode-electrolyte equivalent model is presented along with measurement results.

The wireless energy harvester demonstrates a two-coil system for data and power transfer, unlike conventional four-coil approach [9]. It can recover approximately 1.4mW at 10mm coil separations, while actuating a 10KΩ load. Stimulation range of 2 µA to 200µA is possible with adjustable rate of up to 400Hz. The amplifier has the gain of 1200 and bandwidth from 350Hz to 1.02KHz. Stimulation artifacts are shown to be reduced down to 3ms. The quiescent power of the system is 360µW. An additional 90µW is utilized during 100Hz stimulation rate. The system is applicable to in-vivo experiments and possible implantable prosthesis, such as to treat epileptic seizures.

Acknowledgement

We would like to thank Tata Consultancy Services for providing funds.

References

[1]. Guyton A.C., Hall J. E., "Textbook of Medical Physiology", *Elsevier Saunders*, 11th Ed., 2006.

[2]. Bretschneider F., Weille J. R. de, "Introduction to Electrophysiological Methods and Instrumentation", *Elsevier Acad. Press*, 1st Ed., 2006.

[3]. Pancrazio J.J. et.al., "A portable microelectrode array recording system incorporating cultured neuronal networks for neurotoxin detection", *Biosen. and Bioelect.* vol. 18, pp. 1339-1347, 2003.

[4]. Pliquett U. et al., "Testing miniaturized electrodes", *J Electr. Bioimp.*, vol. 1, pp. 41-55, 2010.

[5]. Brown E.A. et.al., "Stimulus-Artifact Elimination in a Multi-Electrode System", *IEEE Tran. Biomed. Cir. and Sys.*, vol. 2, no. 1, Mar 2008.

[6]. Alvarez I. et.al., "Generalized alternating stimulation: A novel method to reduce stimulus artifact in electrically evoked compound action potentials", *J. Neurosci. Methods*, vol. 165, pp. 95–103, 2007.

[7]. Baker M.W. et.al., "Feedback analysis and design of RF power links for low power Bionic systems", *IEEE Tran. Biomed. Cir. and Sys.*, vol. 1, no. 1, pp. 28-38, Mar. 2007.

[8]. RamRakhyani A.K. et.al., "Design and Optimization of Resonance-Based Efficient Wireless Power Delivery Systems for Biomedical Implants", *IEEE Tran. Biomed. Cir. and Sys.*, vol. 5, no. 1, pp. 48-63, Feb. 2011.

[9]. Shire D.B. et.al., "Development and Implantation of a Minimally Invasive Wireless Subretinal Neurostimulator", *IEEE Tran. Biomed. Engg.,* vol. 56, pp. 2502-2511, Oct. 2009.

[10]. Wheeler H.A., "Formulas for the skin effect", *Proceedings of the I.R.E.,* vol. 30, pp. 412-424, Sept. 1942.

[11]. Wichmann T., "A digital averaging method for removal of stimulus artifacts in neurophysiologic experiments", *J. Neurosci. Methods,* vol. 98, pp. 57–62, 2000.

[12]. Sit J.J. et.al., "A Low-Power Asynchronous Interleaved Sampling Algorithm for Cochlear Implants That Encodes Envelope and Phase Information", *IEEE Tran. Biomed. Engg.,* vol. 54, pp. 138-149, Jan. 2007.